

Efficient computation of the structural phase behavior of block copolymers

G. Tzeremes,* K. Ø. Rasmussen,† T. Lookman, and A. Saxena

Theoretical Division and Center for Nonlinear Studies, Los Alamos National Laboratory, Los Alamos, New Mexico 87545

(Received 21 November 2001; published 10 April 2002)

A numerical implementation of self-consistent mean-field theory for the structural phase behavior of block copolymers is proposed. Our scheme does not require *a priori* assumptions of the underlying mesoscopic symmetries. The method potentially enables us to characterize, with high accuracy, the structural phase diagram of block copolymers with significant architectural complexity. We illustrate the method by applying it to a triblock copolymer system.

DOI: 10.1103/PhysRevE.65.041806

PACS number(s): 61.25.Hq, 64.60.Cn, 64.75.+g

Block copolymers have received considerable attention, both experimentally and theoretically, due to their fascinating ability to self assemble into a variety of ordered nanoscale morphologies [1]. Recently, self-assembled ordered structures with periodicities on the nanometer scale have become an important area of study because of their application in nanotechnology. For instance the self-assembled structures of block copolymers have been used in various templating functions: for nanoscale colloidal particles [2], surface patterning [3], and the creation of photonic band-gap materials [4]. The attractiveness of block copolymer systems is further enhanced by the existence of a quantitative self-consistent mean-field theory (SCMFT) establishing a relation between molecular architecture, composition, and equilibrium self assembly. The SCMFT for polymers originates from the work of Edwards and was later adapted to describe self assembly by Helfand and others [5].

Currently, two efficient numerical approaches to solving the SCMFT exist; (1) Matsen and Schick [6] put forward an approach which involves expanding all spatially extended fields in a finite set of basis functions adapted to an assumed symmetry. Although this method is numerically efficient for a precise calculation of free energies and phase diagrams, it demands that the symmetries of the phases be known. This information is typically lacking in exploratory studies of composite block copolymer materials of different architecture. (2) Drolet and Fredrickson [7] have recently suggested an alternative numerical approach which requires no prior knowledge of symmetry relations. This approach has been applied in a number of studies [8,9]. In this paper we propose a method that does not require *a priori* knowledge of symmetry and (i) is numerically table and (ii) is significantly faster. Our resolution of these issues truly enables a full calculation of structures so that SCMFT can be used in exploratory studies for combinatorial screening.

We first briefly describe the SCMFT for a monodispersed melt of n ABC triblock copolymers. Each triblock molecule is composed of N segments of which $f_A N$, $f_B N$, and $f_C N = (1 - f_A - f_B)N$ form the A , B , and C blocks, respectively.

The interaction between dissimilar blocks, within the SC-MFT, is determined by the three *Flory-Huggins* parameters χ_{AB} , χ_{AC} , and χ_{BC} . In SCMFT the three static fields $\omega_A(\mathbf{r})$, $\omega_B(\mathbf{r})$, and $\omega_C(\mathbf{r})$ represent the molecular interaction acting on A , B , and C , respectively. Denoting by s the contour length (scaled by N) of the copolymer we can, within the above mean-field assumption, write down the exact partition function $\mathcal{Z} = \int d\mathbf{r} q(\mathbf{r}, 1)$ in terms of the statistical weight $q(\mathbf{r}, s)$ that a segment of a chain with the free end ($s=0$) of the A block has its s th segment at \mathbf{r}

$$q(\mathbf{r}, s) = \int \mathcal{D}r_\alpha \delta[\mathbf{r} - \mathbf{r}_\alpha(s)] \times \exp \left[- \int_0^s d\tau \left(\left| \frac{d\mathbf{r}_\alpha(\tau)}{d\tau} \right|^2 + \omega[\mathbf{r}_\alpha(s), s] \right) \right]. \quad (1)$$

Here lengths are in units of the unperturbed radius of gyration R_g of the chain and the subscript α denotes components. The two terms in the statistical weight function represent the entropic penalty for stretching and the energy arising from the static fields, respectively. The field ω for a linear triblock copolymer is defined by

$$\omega(\mathbf{r}, s) = \begin{cases} \omega_A(\mathbf{r}), & \text{for } 0 < s < f_A, \\ \omega_B(\mathbf{r}), & \text{for } f_A < s < f_A + f_B, \\ \omega_C(\mathbf{r}), & \text{for } f_A + f_B < s < 1. \end{cases} \quad (2)$$

For computations $q(\mathbf{r}, s)$ is conveniently determined by the modified diffusion equation

$$\frac{\partial q(\mathbf{r}, s)}{\partial s} = \nabla^2 q - \omega(\mathbf{r}, s) q, \quad (3)$$

with the boundary condition $q(\mathbf{r}, 0) = 1$ [5]. Since the two ends of the copolymer are distinct, a second segment distribution function $q^\dagger(\mathbf{r}, s)$ is defined similarly to q and satisfies the modified diffusion equation

$$-\frac{\partial q^\dagger(\mathbf{r}, s)}{\partial s} = \nabla^2 q^\dagger - \omega(\mathbf{r}, s) q^\dagger, \quad (4)$$

*Present address: Department of Electrical and Computer Engineering, University of New Mexico, Albuquerque, New Mexico 87131-1356

†Corresponding author. Electronic address: kor@lanl.gov

with the boundary condition $q^\dagger(\mathbf{r},1)=1$ [5]. In terms of these distribution functions the monomer densities $\phi_\kappa(\mathbf{r})$ ($\kappa=A, B, \text{ or } C$) become

$$\phi_\kappa(\mathbf{r}) = \frac{V}{\mathcal{Z}} \int_{s_l}^{s_u} ds \, q(\mathbf{r},s) q^\dagger(\mathbf{r},s), \quad (5)$$

where V is the volume (in units of R_g), $s_l=0$, f_A, f_A+f_B , and $s_u=f_A, f_A+f_B, 1$ for $\kappa=A, B, C$, respectively.

The free-energy F per chain (in units of $k_B T$) in terms of the defined quantities is

$$F = -\ln\left[\frac{\mathcal{Z}}{V}\right] + \frac{N}{2V} \sum_{\kappa, \kappa', \kappa \neq \kappa'} \left[\chi_{\kappa\kappa'} \int d\mathbf{r} \phi_\kappa \phi_{\kappa'} \right] - \frac{1}{V} \sum_{\kappa} \left[\int d\mathbf{r} \omega_\kappa \phi_\kappa \right]. \quad (6)$$

Minimization of this free energy with respect to ϕ_κ and ω_κ yields

$$\omega_\kappa = N \sum_{\kappa' \neq \kappa} \chi_{\kappa, \kappa'} \phi_{\kappa'}(\mathbf{r}) + \xi(\mathbf{r}), \quad (7)$$

where $\xi(\mathbf{r})$ is the Lagrange multiplier enforcing the incompressibility constraint $\sum_\kappa \phi_\kappa(\mathbf{r}) \equiv 1$.

Equations (3), (4), and (7) and the corresponding slightly simpler equations for diblock copolymers have been successfully solved by Matsen and Schick [6], Matsen [10], and Laradji *et al.* [11] using a restricted Fourier basis that appropriately represents assumed morphological symmetries. These studies have theoretically determined the phase diagram for diblock copolymers [6] and explored parts of the larger and more complex phase diagram for symmetric triblock copolymers. Particularly, for the more exploratory research on triblock and copolymer systems of similar or higher degree of architectural complexity, this approach has the flaw that the relevant morphologies need to be known *a priori*. To circumvent this problem Drolet and Fredrickson [7] recently suggested an implementation where low free-energy morphologies are found by relaxation from random potential fields.

We now describe our approach to this problem. First, an initial guess for the static fields $\omega_\kappa(\mathbf{r})$ is obtained using a standard random number generator. Thereafter, Eq. (7) combined with the incompressibility relation yields the density fields $\phi_\kappa(\mathbf{r})$ and the Lagrange multiplier $\xi(\mathbf{r})$. Now the modified diffusion Eqs. (3) and (4), are solved to determine $q(\mathbf{r},s)$ and $q^\dagger(\mathbf{r},s)$ for $0 \leq s \leq 1$ and the results are used in Eq. (5) to obtain expressions for the densities $\phi_\kappa(\mathbf{r})$. In principle, the fields $\omega_\kappa(\mathbf{r})$ for the next iterations should be straightforwardly obtained from Eq. (7). However, this approach leads to various convergence problems. Therefore, the authors of Ref. [7] used a linear mix of new (present iteration) and old (previous iteration) density fields $\phi_\kappa(\mathbf{r})$ in Eq. (7) rather than the straightforward approach. In our implementation this leads in almost all cases to a catastrophic instability as the equilibrium solution is iteratively

approached [12]. Inspired by related work [11] we therefore use the following set of equations to obtain the fields $\omega_\kappa(\mathbf{r})$ for the next iteration:

$$\omega_\kappa^{i+1}(\mathbf{r}) = \omega_\kappa^i(\mathbf{r}) + \gamma \delta \omega_\kappa^i(\mathbf{r}) - \epsilon \delta \phi^i(\mathbf{r}), \quad (8)$$

where i is an iteration index and γ, ϵ are small positive numbers [13]. The remaining quantities are defined as

$$\delta \omega_\kappa^i(\mathbf{r}) = N \sum_{\kappa' \neq \kappa} \chi_{\kappa, \kappa'} \phi_{\kappa'}^i(\mathbf{r}) + \xi^i(\mathbf{r}) - \omega_\kappa^i(\mathbf{r}), \quad (9)$$

and

$$\delta \phi^i(\mathbf{r}) = \sum_{\kappa} \phi_\kappa^{i-1}(\mathbf{r}) - \sum_{\kappa} \phi_\kappa^i(\mathbf{r}). \quad (10)$$

The crucial difference compared to the work of Ref. [7] is the last term in Eq. (8) which we found stabilizes the iterations in all cases. Note that this term does not alter the equilibrium state since it vanishes as the fixed point of the iterations is approached. The final step is to update the Lagrangian multiplier $\xi(\mathbf{r})$ combining Eq. (7) with the incompressibility constraint [14]. This procedure is embedded in a minimization procedure wherein the free energy of the structures is minimized with respect to the size of simulation box [15]. As is well known, the true minimum of the free energy is realized only when the box size is commensurate with the periodicity of the equilibrium morphologies. Although this effect clearly diminishes as the simulation box becomes larger, it is advantageous to constrain the size of the simulation box to not exceed two periods as both computation time and the time required to achieve appropriate annealing increase dramatically with the size of the system [7].

Clearly, the main computational effort in the described algorithm resides in solving the modified diffusion Eqs. (3) and (4). The authors of Ref. [7] used a Crank-Nicholson scheme where the severe constraint on spatial and temporal resolutions, imposed by stability requirements, are well known [16]. Rather than using this method or similar finite difference methods we apply a pseudo spectral method and gain about an order of magnitude in computing time for comparable numerical accuracy. Specifically, we use a *split-step Fourier* algorithm [17] achieving its attractiveness for the present problems via the following two virtues: (1) It applies the well-developed fast-fourier transform (FFT), and (2) the two separate steps can be solved exactly allowing coarse resolution along the s direction. Attempting to apply the split-step Fourier algorithm, to solve Eqs. (3) and (4) we observe that a formally exact solution to Eqs. (3) (for $s < f_A$) is

$$q(\mathbf{r}, s+ds) = \exp[ds(\nabla^2 - \omega_A(\mathbf{r}))] q(\mathbf{r}, s). \quad (11)$$

Accepting an error of order ds^3 , Eq. (11) becomes [18]

$$q(\mathbf{r}, s + ds) = \exp\left[-\frac{ds}{2}\omega_A(\mathbf{r})\right] \exp[ds\nabla^2] \\ \times \exp\left[-\frac{ds}{2}\omega_A(\mathbf{r})\right] q(\mathbf{r}, s). \quad (12)$$

Equation (12) can be numerically implemented exactly for a given spatial discretization. The operator $\exp[-ds/2\omega_A(\mathbf{r})]$ is trivially implemented while the operator $\exp(ds\nabla^2)$ is implemented exactly in the spatial Fourier domain. This last step requires one forward and one backward (inverse) FFT representing the main time cost of the approach. The fact that we can implement Eq. (12) exactly allows us to use $ds \sim 0.01$ which is at least an order of magnitude larger than what is possible with a Crank-Nicholson or similar type schemes. This scheme enables simulations of spatial size $\sim (15R_g)^3$ to $(20R_g)^3$ on desktop computers.

To demonstrate the efficiency of our algorithm we consider a triblock system that has been studied by Matsen using a spectral approach [10]. We take an ABC system with symmetric end blocks where $f \equiv f_A = f_C$ and $\chi \equiv \chi_{AB} = \chi_{BC}$. This particular class of ABC triblocks is characterized by just three quantities f , χN , and χ_{AC}/χ . We examine three points in this phase diagram: The three density fields describing the lowest free energy configuration at $(f, \chi N, \chi_{AC}/\chi) = (0.12, 50, 1)$ are shown in Fig. 1. We depict the actual size of the simulated system which is discretized into a $64 \times 64 \times 64$ grid. The figure shows the projection of the density fields on the surfaces depicted with red color indicating high density (~ 1) and with blue color indicating low density (~ 0) regions. As shown by Matsen [10], we find that the lowest-energy configuration at this point of the phase diagram is a body-centered-cubic (bcc) structure in the sense that both ϕ_A and ϕ_C fields form cubic structures but displaced in space such that the combined field $\phi_A + \phi_C$ forms the bcc structure. The free energy of this structure is $F = 9.275$ and the lattice parameter of the cubic structure is $D = 3.4R_g$, consistent with Ref. [10].

Figure 2 shows the minimum free-energy configuration at $(f, \chi N, \chi_{AC}/\chi) = (0.14, 50, 1)$, which in this case consists of hexagonally packed cylinders. Again, the hexagonal packing occurs in the combined field $\phi_A + \phi_C$ while the individual fields show cubic packing. As this method starts from a random initial condition we have, contrary to the spectral method, no control over the orientation of the resulting morphology. This is clearly seen in this example, the cylinders misalign with the box axes. The free-energy of this structure is $F = 9.58$ and the lattice parameter of the hexagonal pattern is $D = 4.1R_g$, again consistent with Ref. [10]. Finally, Fig. 3 displays the minimum free energy configuration at $(f, \chi N, \chi_{AC}/\chi) = (0.25, 50, 1)$ consisting of a lamellar morphology. In this particular configuration the free energy of the structure is $F = 9.726$ and the period of the lamellar modulation is $D = 7.4R_g$, which is quite large for a method like this to handle successfully. Moreover, we have also found a gyroid structure in the regions of the phase diagram where Ref. [10] indicates its presence.

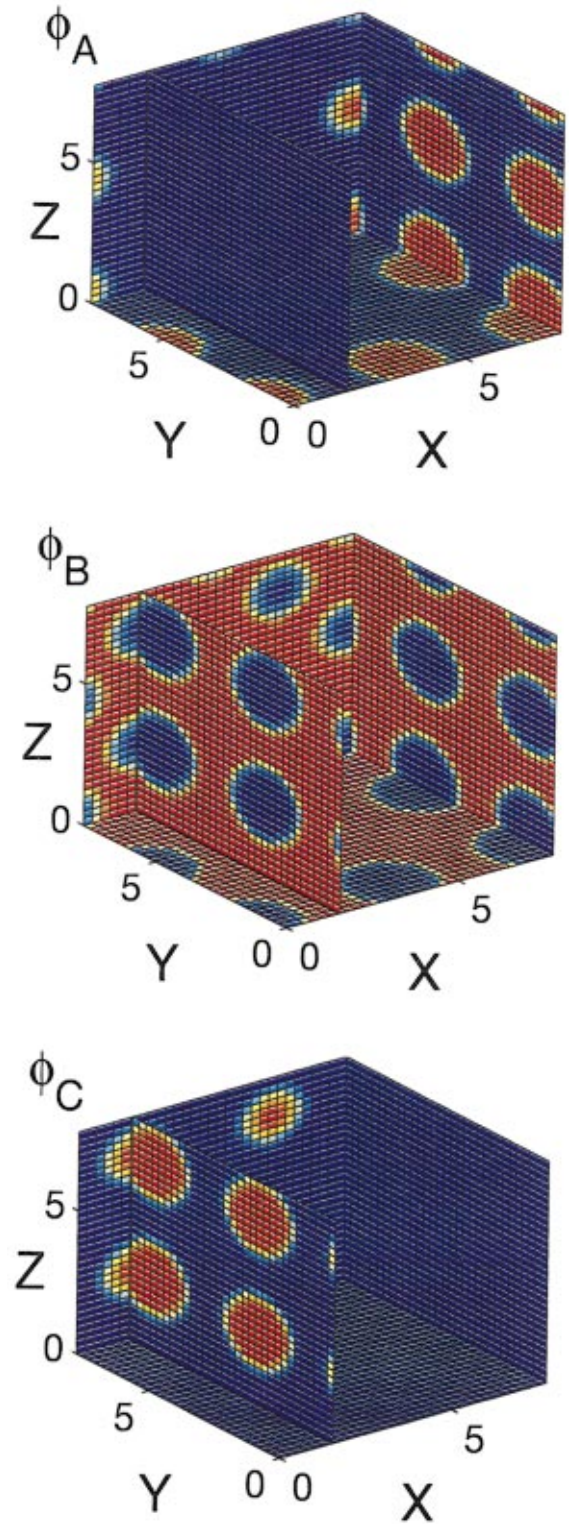


FIG. 1. (Color) Three-dimensional density plot of the minimum energy phase (bcc structure) at $(f, \chi N, \chi_{AC}/\chi) = (0.12, 50, 1)$. The three densities are separately shown as projections on the depicted surfaces with the color red indicating high density and the color blue indicating low density. Distances are in units of R_g .

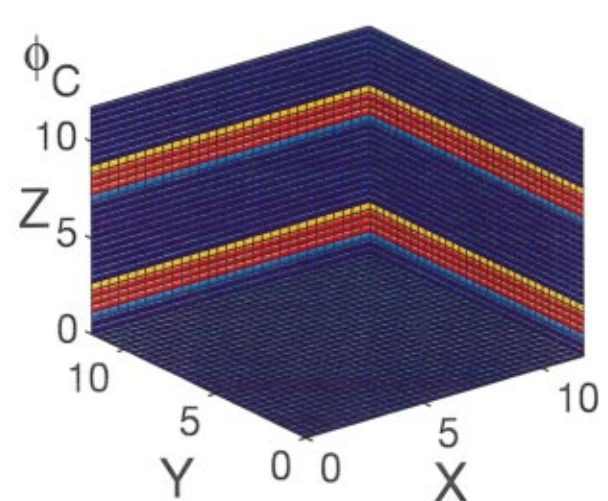
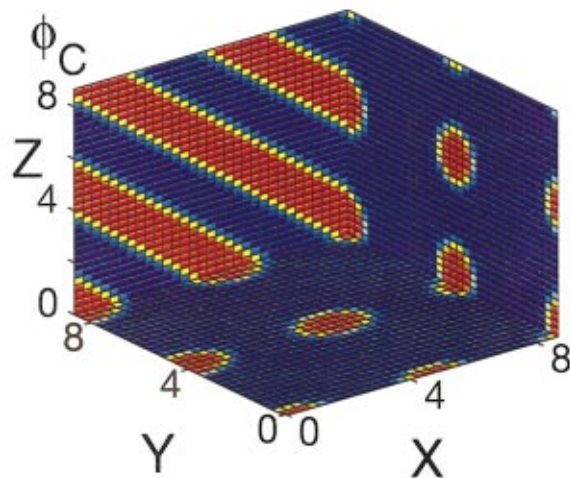
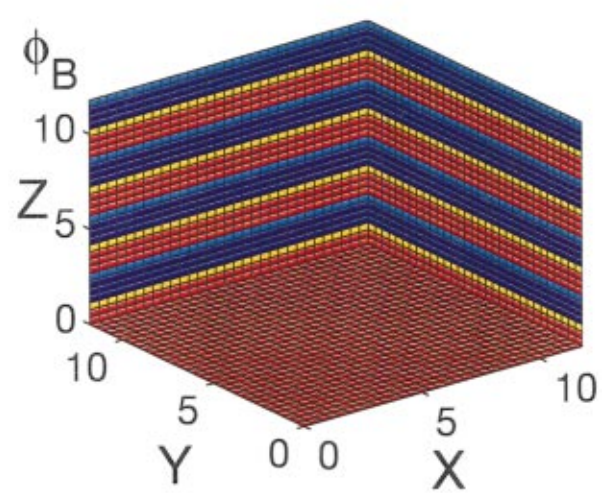
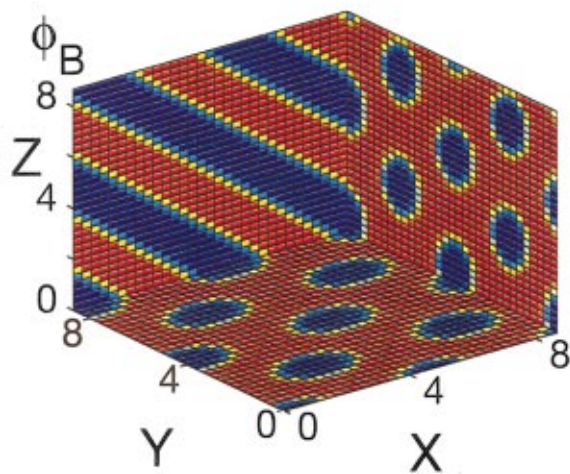
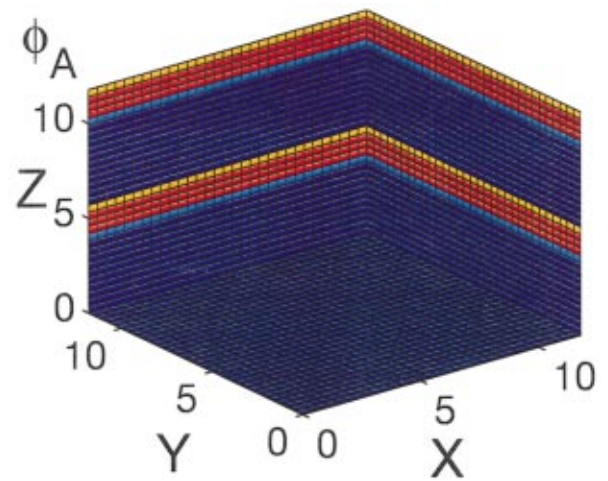
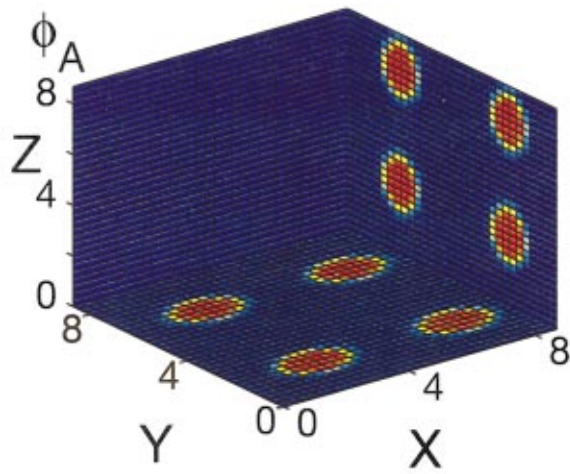


FIG. 2. (Color) Three-dimensional density plot of the minimum energy phase (hexagonally packed cylinders) at $(f, \chi N, \chi_{AC}/\chi) = (0.14, 50, 1)$. The three densities are separately shown as projections on the depicted surfaces with the color red indicating high density and the color blue indicating low density. Distances are in units of R_g .

FIG. 3. (Color) Three-dimensional density plot of the minimum energy phase (lamellar structure) at $(f, \chi N, \chi_{AC}/\chi) = (0.25, 50, 1)$. The three densities are separately shown as projections on the depicted surfaces with the color red indicating high density and the color blue indicating low density. Distances are in units of R_g .

In summary, we have presented a numerical algorithm to solve the SCMFT for block copolymer systems which is numerically superior in stability and performance to existing approaches. We applied it to study the morphologies of a triblock copolymer. This method represents an important advance for the applicability of the SCMFT as a combinatorial

screening technique in future exploratory materials science of block copolymers and nanoscale composite systems.

We acknowledge fruitful discussions and interactions with Professor Rashmi Desai. Work at Los Alamos National Laboratory is performed under the auspices of the US Department of Energy.

-
- [1] I. W. Hamley, *The Physics of Block Copolymers* (Oxford University Press, New York, 1998).
- [2] T. Sato, D.G. Hasko, and H. Ahmed, *J. Vac. Sci. Technol. B* **15**, 45 (1997).
- [3] M. Böltau, S. Walheim, J. Mlynek, G. Krausch, and U. Steiner, *Nature (London)* **391**, 877 (1998).
- [4] M. Srinivasarao, D. Collings, A. Philips, and S. Patel, *Science* **292**, 79 (2001).
- [5] S.F. Edwards, *Proc. Phys. Soc. London* **85**, 613 (1965); E. Helfand, *J. Chem. Phys.* **62**, 999 (1975); E. Helfand and Z.R. Wasserman, *Macromolecules* **9**, 879 (1976); K.M. Hong and J. Noolandi, *ibid.* **14**, 727 (1981); J.D. Vavasour and M.D. Whitmore, *ibid.* **25**, 5477 (1992).
- [6] M.W. Matsen and M. Schick, *Phys. Rev. Lett.* **72**, 2660 (1994).
- [7] F. Drolet and G.H. Fredrickson, *Phys. Rev. Lett.* **83**, 4317 (1999).
- [8] R.B. Thompson, V.V. Ginzburg, M.W. Matsen, and A.C. Balazs, *Science* **292**, 2469 (2001).
- [9] F. Drolet and G.H. Fredrickson, *Macromolecules* **34**, 5317 (2001).
- [10] M.W. Matsen, *J. Chem. Phys.* **108**, 785 (1998).
- [11] M. Laradji, A.-C. Shi, R.C. Desai, and J. Noolandi, *Phys. Rev. Lett.* **78**, 2577 (1997) and references therein.
- [12] The catastrophic instability also appeared in the simpler case of diblock copolymers and seems unrelated to the increased complexity of triblock copolymers.
- [13] We generally used $0.1 \leq \gamma, \epsilon \leq 0.2$ noting that the larger values (of particularly γ) allow faster convergence.
- [14] In the triblock case the Lagrangian multiplier is given by $\xi(\mathbf{r}) = (2N\chi_{AB}\chi_{BC}\chi_{AC} - \sum_{\kappa} \omega_{\kappa}(\mathbf{r})X_{\kappa}) / \sum_{\kappa} X_{\kappa}$, where $X_A = \chi_{BC}(\chi_{AB} + \chi_{AC} - \chi_{BC})$, $X_B = \chi_{AC}(\chi_{BC} + \chi_{AB} - \chi_{AC})$, and $X_C = \chi_{AB}(\chi_{AC} + \chi_{BC} - \chi_{AB})$.
- [15] Y. Bohbot-Raviv and Z.-G. Wang, *Phys. Rev. Lett.* **85**, 3428 (2000).
- [16] A. R. Mitchell and D. F. Griffiths, *The Finite Difference Method in Partial Differential Equations* (Wiley, Chichester, 1980).
- [17] R.H. Hardin and F.D. Tappert, *SIAM Rev.* **15**, 423 (1973); R.A. Fisher and W.K. Bischel, *Appl. Phys. Lett.* **23**, 661 (1973); *J. Appl. Phys.* **46**, 4921 (1975); J.A. Fleck, J.R. Morris, and M.D. Feit, *Appl. Phys.* **10**, 129 (1976).
- [18] This result is obtained by applying the Baker-Hausdorff operator identity [see, e.g. G.H. Weiss and A.A. Maradudin, *J. Math. Phys.* **3**, 771 (1962)] $\exp(ds\nabla^2)\exp(-ds\omega_A) = \exp(ds\nabla^2 - ds\omega_A - ds^2/2[\nabla^2, \omega_A] - ds^3/12[\nabla^2 + \omega_A, [\nabla^2, \omega_A]] + \dots)$ twice, whereby the terms of order ds^2 vanish identically leaving only terms of order ds^3 and higher. $[\nabla^2, \omega_A] = \nabla^2\omega_A - \omega_A\nabla^2$ denotes the standard commutator.